



## Exploresearch

Impact Factor (Cosmos: 6.262& I2OR: 3.585)

© Copyright by MGM Publishing House (MGMPH)

www.mgmpublications.com



# A Comparative Analysis of Land Use and Land Cover (LULC) Changes in the Indian and Bangladeshi Sundarbans using Remote Sensing

Hitanshu Biswas<sup>1\*</sup> & Dr. Deepak Kumar Sharma<sup>2</sup>

<sup>1</sup>Research Scholar, Nirwan University Jaipur & Assistant Professor in Environmental Science, Kabi Nazrul College, Murarai, Birbhum, West Bengal.

<sup>2</sup>Associate Professor, School of Basic and Applied Science, Nirwan University Jaipur, Rajasthan, India.

\*Corresponding author: hitangshuu@gmail.com

**Citation:** Biswas, H. & Sharma, D. (2026). A Comparative Analysis of Land Use and Land Cover (LULC) Changes in the Indian and Bangladeshi Sundarbans using Remote Sensing. *Exploresearch*, 03(01), 206–213.  
<https://doi.org/10.62823/ExRe/2026/03/01.190>

### Article History:

**Received:**01 March 2026

**Revised:**16 March 2026

**Accepted:**24 March 2026

**Published:**31 March 2026

### Keywords:

Land Use Land Cover Changes, Indian Sunderbans, Sundarbans, Bangladesh Sundarbans, Water Bodies, Dense Forest, Cyclones, Agricultural Land, Anthropogenic Activities.

**Abstract:** The Sundarbans (also spelled Sunderbans) is the world's largest mangrove forest, spanning approximately 10,000 km<sup>2</sup> across India (about 38%) and Bangladesh (62%). It features dense mangrove vegetation, tidal waterways, mudflats, and islands critical for biodiversity, coastal protection, and livelihoods. Land cover has changed significantly over decades, tracked primarily through Landsat satellite imagery and GIS analysis. The core mangrove forest shows degradation in density (dense areas converting to sparser vegetation or water), driven by erosion, sea-level rise, cyclones, and human pressures, though the overall extent remains relatively stable in protected core zones with signs of natural resilience in some areas. Dense mangroves mainly transitioned to moderate/sparse categories; sparse areas often became barren or inundated. Accuracy of classifications: 85–90% (kappa 0.81–0.87). Bangladesh portion (core protected area): Mangrove Forest cover remained largely stable overall, with minor bank/coastline erosion. Surrounding non-forested areas were converted to water bodies due to shrimp farming and aquaculture. Indian portion (more impacted near human settlements): Greater increase in sparse/barren land. Shoreline analysis (1980–2021) shows a net land loss of ~152 km<sup>2</sup> (243 km<sup>2</sup> eroded vs. 91 km<sup>2</sup> accreted). Erosion dominated eastern/southern lobes and southern sea-facing islands; western areas were more dynamic. This depleted moderate vegetation by ~174 km<sup>2</sup> (sparse gained slightly from accretion but overall vegetation suffered). The Sundarbans is losing dense mangrove cover and land area (especially in India), converting to sparser vegetation, barren zones, or water—but the ecosystem shows some resilience and recovery potential through regeneration. Protected status and reforestation have helped stabilize parts of it. Ongoing monitoring via satellite remote sensing is essential for

management. This work is based on this remote sensing technique to see land use land cover pattern change over past years. For the latest high-resolution data, tools like Google Earth Engine continue to track these dynamics. Conservation efforts (e.g., mangrove planting, sustainable livelihoods) are critical to counter future sea-level rise and storms.

### Introduction

Our Earth comprises different types of ecosystems, among which mangroves can be considered the most biologically productive. They are present in the tidal zones in tropical and subtropical coastlines, and local temperature conditions have a major role in their forming and maintenance. This research work is based on the largest mangrove forest in the world, which stretches from India to Bangladesh, and it is named the Sundarbans. Mangrove areas around the world have seen a steep decline from 198,000 km<sup>2</sup> in 1980 to 146,530 in 2000 [1]. And the same applies to the Sundarbans region, which is why this study has been undertaken to study changes in land use patterns of the Sundarbans of India and Bangladesh [2, 3].

Sundarbans is the largest contiguous mangrove forest in the world, accounting for 3% of the total global mangrove area. It covers an area of around 10,000 km<sup>2</sup>, out of which about 6200 km<sup>2</sup> (62%) falls in Bangladesh and the rest, 38%, which is 3800 km<sup>2</sup>, comprises Indian mangrove [4]. The mangroves of India and Bangladesh are managed independently now, but they were a single entity until the partition of India in 1947.

The Sundarbans mangroves of both India and Bangladesh are witnessing a steep decline because of both natural and anthropogenic reasons. There are several reasons for this decline, which has been reported to be about 1.2% (1970-2000). Major reasons for decline [5] have been shown in figure 1.

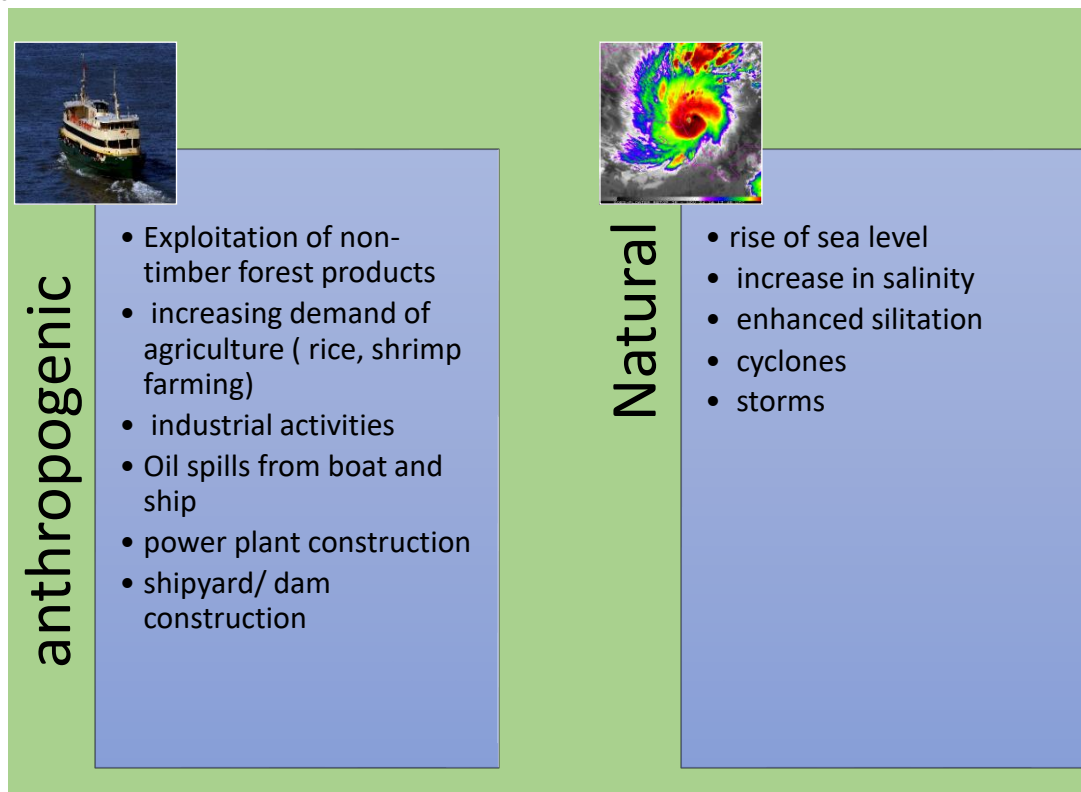


Fig. 1: Major Reasons for the Decline of Sunderbans

### Study Area

In the present work the study area is the entire Sundarbans mangrove, including parts of Bangladesh and India.

### Area Definition

The Sundarbans of India is formed by the rivers Ganges, Brahmaputra, Meghna, and Hooghly in their final journey, towards the Bay of Bengal [6]. These rivers are the main suppliers of fresh water and sediment to the Sunderbans region. Around 30% of the total Sundarbans area is covered by water, and total annual precipitation is up to 2000 mm. The monsoon season is accompanied by several floods, and wind damage is caused by tropical cyclones.

**The area of the Sundarbans in India (the mangrove forest/reserved forest portion in West Bengal) is 4,263 km<sup>2</sup>.** This is the standard official figure for the Indian portion of the world's largest mangrove forest (shared with Bangladesh). It includes land and extensive water bodies (rivers, creeks, and canals, which make up roughly 1,700–1,874 km<sup>2</sup>).

### Important aspects of the Indian Sunderban

- **Total Sundarbans (India + Bangladesh):** ~10,000–10,277 km<sup>2</sup>.
- **Indian Sundarbans Forest area:** ~ 4,263 km<sup>2</sup> (official West Bengal/Sundarban Tiger Reserve annual report).
- **Sundarban Tiger Reserve** (core protected area): 2,585 km<sup>2</sup> (being expanded by ~1,044 km<sup>2</sup> to become one of India's largest tiger reserves).
- **Sundarbans National Park** (UNESCO World Heritage core): 1,330 km<sup>2</sup>.
- **Indian Sundarbans Biosphere Reserve** (broader region including non-forest areas): ~9,630 km<sup>2</sup>.
- **Ramsar Wetland designation** (Sundarban Wetland, 2019): 423,000 ha = 4,230 km<sup>2</sup> (very close to the forest figure).

These numbers come from official Indian government sources (Sundarban Tiger Reserve reports), UNESCO, and Ramsar records. The exact figure can vary slightly by source.

### The Sundarbans in Bangladesh covers approximately 6,017 km<sup>2</sup> (2,323 sq. mi)

This is the Bangladeshi portion of the world's largest mangrove forest (located in Khulna Division), which forms part of the total Sundarbans spanning India and Bangladesh. The overall area is around 10,000–10,277 km<sup>2</sup>, with roughly 60% (about 6,000 km<sup>2</sup>) in Bangladesh and the rest in India's West Bengal.

### Methodology

This study was based on satellite images [8] obtained from various sensors for the time period of 1975-2020. A five-step process (fig. 2) was applied in the study, which are briefly described as below:

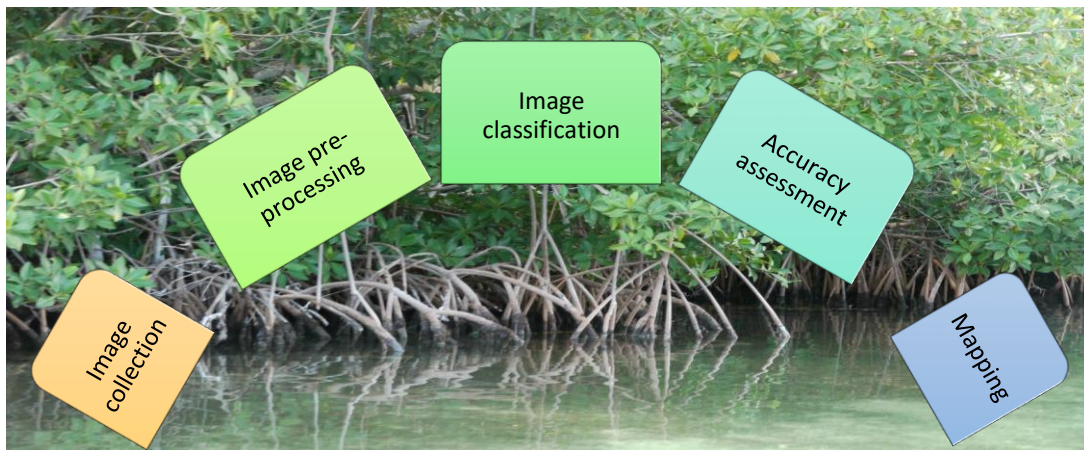


**Fig. 2: Remote Sensing and Related Methods used in this Study**

### Image Collection

Landsat satellite collection-1 level-1 images [6] are famous for being the best in quality to support time series analysis, according to the United States Geological Survey, 2019. Most of the images were cloud-free (Table 1). These were acquired from January to February because this is the winter season, having cold/dry condition conditions and number of fewer clouds in the Sunderbans regions is less.. 2020 images were obtained by Operational Land Imager and Thermal Infrared Sensor.

**Table 1.** Source and specification of satellite images used in the study.

Year	Data acquisition date/time	SatelliteSensor	Path/ Row	Used bands	Spatial resolution	Cloud cover	Covered area*
1975	19 February 1975	L 2/MSS	147/045	4-7	60 m	0%	BS
	10 January 1976	L 2/MSS	148/045	4-7	60 m	0%	IS, BS
	10 January 1976	L 2/MSS	148/044	4-7	60 m	0%	BS
1990	24 February 1990	L 5/TM	137/045	1-7	30 m	0%	BS
	14 January 1990	L 5/TM	138/045	1-7	30 m	0%	IS, BS
2005	16 January 2005	L 5/TM	137/045	1-8	30 m	0%	BS
	7 January 2005	L 5/TM	138/045	1-8	30 m	0%	IS, BS
	26 January 2020	L 8/OLI	137/045	1-7	30 m	0%	BS
2020	Jan 17, 2020	L 8/OLI	138/045	1-7	30 m	0.62%	IS, BS

Covered area\*: BS = Bangladesh Sunderbans, IS = Indian Sunderbans

### Image Pre-Processing

Collected images were subjected to atmospheric and radiometric correction with the help of Fast Line-of-Sight Atmospheric Analysis Hypercubes (FLAASH) in ENVI 5.3 [9]. This is a highly specific and widely used atmospheric correction algorithm working in remote sensing [10]. Despite being a time-consuming process, this method is favoured because of its accuracy [11]. The flash model works on a combination of 2 equations that help to minimise atmospheric elements like water vapour, smog, fog, and dust, and the aerosol effect in images. Equation 3 was used for image rectification, along with 50 ground control points. In a study conducted by Hossain et al. (2024) [25], the root mean square error was 0.39, which was in the acceptable range for detecting land-use land-cover change. The images were then resampled to a 30 m pixel size using the nearest neighbour resampling method [12].

### Image Classification

It was achieved by using supervised maximum likelihood classification on the study area for 4 time periods. The classification was subdivided into five classes [13]. Namely, forest cover that included dense, moderate, and sparse forests; barren land; and water. This algorithm was used because it is easy to use and does not require an extended training process. Also, it is able to extract detailed information by calculating the weighted distance or likelihood of an unknown measurement vector that comes under one of the known classes based on the Bayesian equation.

Also, in this type of algorithm, an unknown measurement vector is assigned to that class, which has the highest probability of fit. A major advantage of using this algorithm is that it considers the variance-covariance matrix within the class distribution. Alongside superior classification, it is definitely dependent on enough numbers of training samples to satisfy this required requirement [14]. In a study conducted by Hossain et al. (2024) [25], which is the basic sample paper used in this study, 245 training samples were identified for LULC classes [15, 16]. Different colours were assigned for the representation of water, and it was done because of water having different colours at the coast, beach, shoreline, and deep river basins. Different types of water bodies sites were considered for training samples, which were selected manually. High-resolution Google Earth images were used as a reference point.

### Accuracy Assessment

From amongst the hundred control points, 250 control points were chosen on a random basis over the classified images. Each point was given a label depending upon the 30 m radius of land cover around it. Classification accuracy was then calculated by taking care of the error matrix producer user. And overall accuracy end with the help of the kappa coefficient (K), and a higher value of K [17] was indicative of higher accuracy of LULC.

### Mapping

Upon completion of the accuracy assessment, final mapping [18] was conducted to find out different LULC types. Overall, the accuracy rate was found to be between 84.8% and 90.0%. The highest accuracy on an overall basis was for 2020 (Table 2). The producer's and user's accuracy were maximum

for water. The highest difference between the producer's and user's value was for sparse and moderate forest. Ranges of the kappa coefficient were between 0.81 and 0.87, being highest for the year 2020.

**Table 2.** Analysis accuracy metrics of classified Landsat images of Sundarbans (1975–2020).

Year(Used sensor)	Land use classes										Overall accuracy	Kappa coefficient (K)
	Dense forest		Medium dense forest		Sparse forest		Barren land		Water body			
	PA	UA	PA	UA	PA	UA	PA	UA	PA	UA		
1975 (MSS)	87	84	82	83	81	84	79	83	92	91	84	0.81
1990 (MSS)	88	87	81	87	84	89	88	93	91	90	88	0.85
2005 (TM)	89	90	80	86	82	87	85	90	94	91	87	0.83
2020 (OLI)	88	90	86	88	89	85	80	89	96	93	90	0.87

"PA" and "UA" indicates producer's and user's accuracy respectively

**Discussion**

The land use land cover pattern of dense forest cover was found to be highest around 1975. And since then, it has been steeply declining with very few exceptions, and the overall result is that the dense area has declined with an annual rate of 1.3%. A study conducted by Hossain et al. [25] reported that on one hand dense forest cover was decreasing, but simultaneously moderate and dense forests were found to increase, and the same pattern was observed between sparse and barren land. These thematic changes [19] are indicative of the conclusion (fig. 3) that Sundarbans' dense forest got converted to moderate-density forests and sparse forests. And a large number of sparse forests changed into barren land. Thus, this study justifies its aim of studying land use land cover patterns in the 21st century.

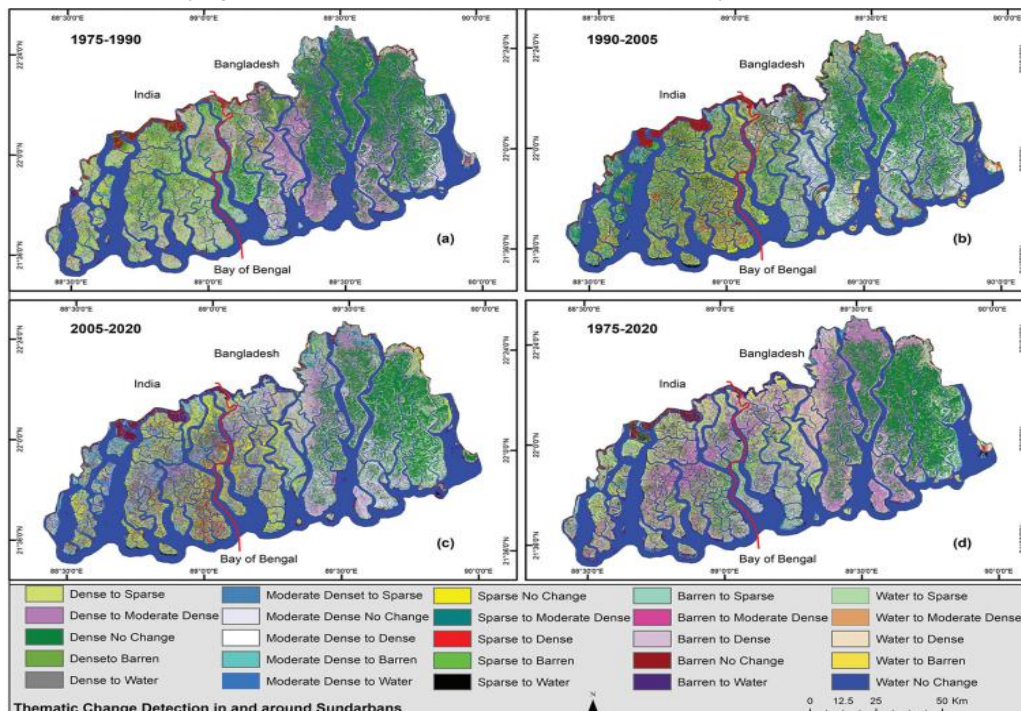


**Fig. 3: Thematic change in Sunderbans from (1975 to 2020)**

There were several reasons for the changing pattern of land use, which include anthropogenic activities [20]. Which means exploiting mangroves and Sundarbans for obtaining items like honey, firewood, thatching material, crab, and medicinal plants; expanding agricultural land, which included shrimp farming and paddy cultivation; and excessive industrialization, which included power plant dam construction [21] and the establishment of ports and shipyards. Several natural factors, including cyclones [22], storms, salinity, siltation, natural pests, and diseases, are a few major culprits. Among the climatic factors, the major one is the rise of the sea level of the Sundarbans [23, 24].

### Significance of Present Study

Land use land cover changes are a means to study and learn about transitions of different land use types and the complex interaction of the physical environment with human beings [1]. A study of land use land cover patterns helps a society to foster sustainable land use planning in order to protect and conserve natural resources and habitats. Major factors that contribute to landscape use and land cover changes of any specific area include precipitation, climate, topography, and anthropogenic factors.

Industrial development in this region, including the construction of dams, is one of the main causes of declining forest cover. In this study, forest cover was greater in the eastern Sunderbans in comparison to other regions (Figure 4). The reason is a decrease of salinity from west to east; this is proved by the presence of the tree *Heritiera fomes*, which is found in regions of less salinity [7]. The coverage of this type of tree has reduced from 32% to 21% in 1983 and further reduced to 17% in 2015 in Bangladesh. Construction of the Rampal power plant is located just 14 km away. The north of Sunderbans is also one of the main reasons for degradation.

Cyclones are a major culprit among natural factors that cause depletion of forests and forest landscapes. Sunderbans was once acting as a natural barrier protecting coastal people and their property from cyclones, tides, and coastal soil erosion. Cyclones have disrupted this natural barrier each year in Bangladesh [26]. The intensity of a cyclone is dependent on speed of wind, distance, connectivity from the eye of the cyclone, precipitation etc. [22]. A recent cyclone, Bulbul (2019), had excessively high wind speed, causing great damage to the Sunderbans. According to Samantha (2021) [27], high and low losses caused by bulbul were 303.6 km<sup>2</sup> and 950.7 km<sup>2</sup> respectively. Cyclone Bulbul also caused great damage in Bangladesh. Two other cyclones, Sider (2007) and Alia (2009), have also caused devastating effects, where Sider was responsible for breaking off trunks of 24% of forests, including uprooting and substrate loss along with local scour around the trees [22].

Land use land cover change in the previous century—Around 1975 dense forests were the category that covered the maximum area, 45% of the Sunderbans (fig. 4); they were followed by water (32%), barren land (10%), moderately dense forests (8%), and sparse forest (5%) (table 3). In land use and land cover change as observed in 2020, the majority of the area was covered by water, and the moderate-dense-forest category fell down in its position. Geospatial photographs exhibited that dense forests were found more in the eastern part, and sparse forest and barren land were mainly found in the Indian part. The highest number of barren land areas was found to be situated at the borderline between forests and human habitation.

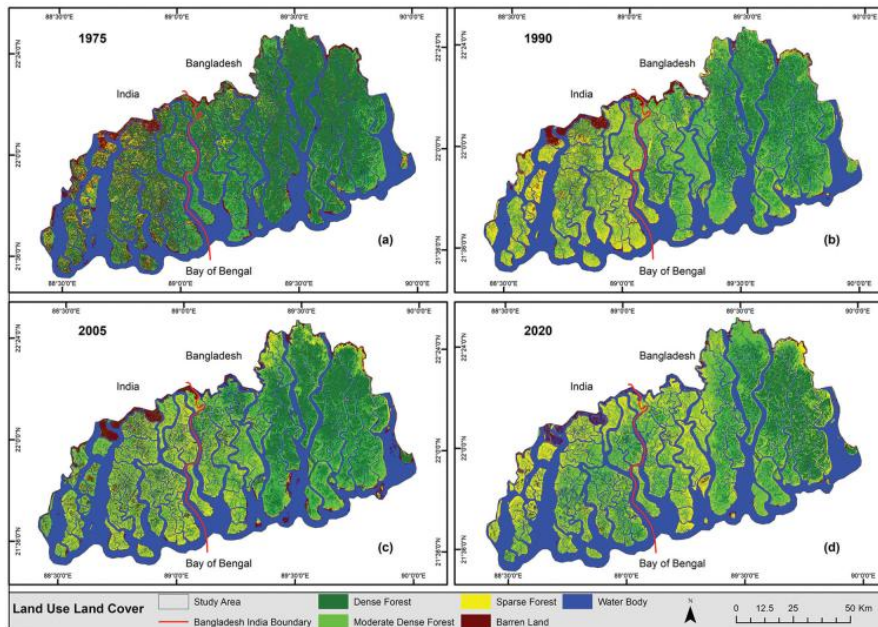


Fig. 4: Land use and Land Cover Changes of Sunderban from 1975 to 2020

**Table 3.** Analysis LULC of Sundarbans (1975–2020).

LULC	Area (km <sup>2</sup> )(% of total area)				Area changes (km <sup>2</sup> )(Annual rate of changes %)			
	1975	1990	2005	2020	1975–1990	1990–2005	2005–2020	1975–2020
Dense forest	4527(45%)	2657(27%)	2818(28%)	1864(19%)	-1870(-2.75%)	+161(+0.40%)	-954(-2.25%)	-2663(-1.30%)
Moderate – dense forest	809(8%)	1817(18%)	1734(17%)	2120(21%)	+1008(+8.31%)	-83(-0.30%)	+386(+1.48%)	+1312(+3.61%)
Sparse forest	530(5%)	1735(17%)	1363(14%)	1815 (18%)	+1205(+15.15%)	-372(-1.43%)	+452(+2.21%)	+1285(+5.39%)
Barren land	1002(10%)	416(4%)	522(5%)	247 (2%)	-585(-3.90%)	+106(+1.70%)	-275(-3.51%)	-754(-1.67%)
Water bodies	3142(32%)	3408(34%)	3596(36%)	3963 (40%)	+266(+0.57%)	+188(+0.37%)	+366(+0.68%)	+821(+0.58%)

"+" and "-" indicates increase and decrease respectively

### Conclusion

The major land use land cover pattern changes, which is the main objective of this work can be concluded as:

There was around 1.3% loss of dense forests per year from 1975 to 2020 (Table 3). But this change was not consistent. The decline of dense forest was 2.75% per year from 1975 to 1990, but it was seen to be 2.25% per year from 2005-2020. There was increase in dense forest at a rate of 0.40% annually from 1990-2005. There was increase in moderate and sparse forest cover from 1975-2020 but there was a decline in these from 1990-2005. Water cover on land showed a steady increase of 0.6% per year from 1975 to 2020; however, the increase was steep in the time frame 2005-2020.

### Thematic Mapping

It represented the pattern (1975-2020) in which dense forest cover changed and the type of change was different in India and Bangladesh. In India barren land got diminished and there was enhancement of dense, moderate and sparse forest cover. But in Bangladesh dense forest cover got reduced and there was seen increase in moderate and sparse forest cover. But one common thing observed was no change in barren land present between human dwelling and forest outskirts. The major thematic change observed was conversion of dense forest cover into water bodies (2.45%), sparse forests (10.41%), and moderately dense forests (15.62) in ascending order. Most change in LULC was seen from dense to moderately dense and sparse forest cover from 1975-90 rather than in 1990-2005 and 2005-2020.

Conflict of Interest—None

\*\* All tables and satellite image figures are from Akbar Hossain, K., Masiero, M., & Pirotti, F. (2024). Land cover change across 45 years in the world's largest mangrove forest (Sundarbans): the contribution of remote sensing in forest monitoring. *European Journal of Remote Sensing*, 57(1). <https://doi.org/10.1080/22797254.2022.2097450>

### References

- Nayak, P.M.; Byrne, M.L. Impact of land use land cover change on a sand dune ecosystem in Northwest Beach, Point Pelee National Park, Canada. *J. Great Lakes Res.* **2019**, *45*, 1047–1054.
- Datta, D., & Deb, S. (2012). Analysis of coastal land use/land cover changes in the Indian Sundarbans using remotely sensed data. *Geo-spatial Information Science*, 15(4), 241–250.
- Hassan, M. M. (2017). Monitoring land use/land cover change, urban growth dynamics and landscape pattern analysis in the five fastest urbanized cities in Bangladesh. *Remote Sensing Applications: Society and Environment*, 7, 69–83.
- Ghosh, A., Schmidt, S., Fickert, T., & Nüsser, M. (2015). The Indian Sundarbans Mangrove forests: History, utilization, conservation strategies, and local perception. *Diversity*, 7(2), 149–169.
- Islam, D. K. M. N. (2010). Integrated Protected Area Co-Management (IPAC) - A Study of the Principal Marketed Value Chains Derived from the Sundarbans Reserved Forest. USAID.
- Bera, S., & Chatterjee, N. D. (2019). Mapping and monitoring of land use dynamics with their change hotspot in North 24-Parganas district, India: A geospatial- and statistical-based approach. *Modeling Earth Systems and Environment*, 5(4), 1529–1551.
- Aziz, A., & Paul, A. R. (2015). Bangladesh Sundarbans: present status of the environment and biota. *Diversity*, 7(3), 242–269.
- Islam, M. M., Borgqvist, H., & Kumar, L. (2019). Monitoring mangrove forest land cover changes in the coastline of Bangladesh from 1976 to 2015. *Geocarto International*, 34(13), 1458–1476.
- Smith, M. J. (2015). A Comparison of DG AComp, FLAASH, and QUAC Atmospheric Compensation Algorithms Using WorldView-2 Imagery. Department of Civil Engineering Master's Report University of Colorado.

10. Serrano, P. M. L., Rivas, J. J. C., Varela, R. A. D., González, J. G. A., & Sánchez, C. A. L. (2016). Evaluation of radiometric and atmospheric correction algorithms for aboveground forest biomass estimation using Landsat 5 TM data. *Remote Sensing*, 8(5), 369.
11. Smith, M. J. (2015). A Comparison of DG AComp, FLAASH and QUAC Atmospheric Compensation Algorithms Using WorldView-2 Imagery. Department of Civil Engineering Master's Report University of Colorado
12. Ghosh, M. K., Kumar, L., & Roy, C. (2016). Mapping long-term changes in mangrove species composition and distribution in the Sundarbans. *Forests*, 7(12), 305. [https](https://doi.org/10.3390/forests7120305)
13. Lu, D., & Weng, Q. (2007). A survey of image classification methods and techniques for improving classification performance. *International Journal of Remote Sensing*, 28(5), 823–870.
14. Kanan, A. H., Pirotti, F., & Masiero, M. (2021). Analysing change dynamics of land cover, erosion and accretion of the world's largest mangrove forest (Sundarbans) using remotely sensed data. 40th EARSeL Symposium, 7-10 June 2021, University of Warsaw, Poland.
15. Chen, C. F., Son, N. T., Chang, N. B., Chen, C. R., Chang, L. Y., Valdez, M., Aceituno, J. L., Thompson, C., & Aceituno, J. (2013). Multi-decadal mangrove forest change detection and prediction in Honduras, Central America, with Landsat imagery and a Markov chain model. *Remote Sensing*, 5(12), 6408–6426.
16. Hasan, M. E., Nath, B., Sarker, A. H. M. R., Wang, Z., Zhang, L., Yang, X., Nobi, M. N., Røskaft, E., Chivers, D. J., & Suza, M. (2020). Applying multi-temporal Landsat satellite data and Markov-cellular automata to predict forest cover change and forest degradation of Sundarban Reserve Forest, Bangladesh. *Forests*, 11(9), 1–35.
17. Stehman, S. V. (1996). Estimating the kappa coefficient and its variance under stratified random sampling. *PE & RS. ASPRS*, 401–407.
18. LaRocque, A., Phiri, C., Leblon, B., Pirotti, F., Connor, K., & Hanson, A. (2020). Wetland mapping with Landsat 8 OLI, Sentinel-1, ALOS-1 PALSAR, and LiDAR data in Southern New Brunswick, Canada. *Remote Sensing*, 12(13), 2095.
19. Li, C., Wang, J., Wang, L., Hu, L., & Gong, P. (2014). Comparison of classification algorithms and training sample sizes in urban land classification with Landsat thematic mapper imagery. *Remote Sensing*, 6(2), 964–983.
20. Billah, M. M., Rahman, M. M., Abedin, J., & Akter, H. (2021). Land cover change and its impact on human– elephant conflict: A case from Fashiakhali Forest Reserve in Bangladesh. *SN Applied Sciences*, 3(6), 649.
21. Das, G. K., & Datta, S. (2016). Man-made environmental degradation at Sunderbans. *Reason-A Technical Journal*, 13, 89.
22. Mandal, M. H. S., & Hosaka, T. (2020). Assessing cyclone disturbances (1988–2016) in the Sundarbans mangrove forests using Landsat and Google Earth Engine. *Natural Hazards*, 102(1), 133–150.
23. Quader, M. A., Agrawal, S., & Kervyn, M. (2017). Multidecadal land cover evolution in the Sundarban, the largest mangrove forest in the world. *Ocean & Coastal Management*, 139, 113–124.
24. Rahman, M. M. (2020). Investigation into the Sea Level Rise as Fallout of Climatic Change: Case Study of the Coast of Bangladesh [M. Phil. Dissertation], University of Dhaka. Retrieved March 7, 2022, from <http://repository.library.du.ac.bd:8080/handle/123456789/1634>
25. Akbar Hossain, K., Masiero, M., & Pirotti, F. (2024). Land cover change across 45 years in the world's largest mangrove forest (Sundarbans): the contribution of remote sensing in forest monitoring. *European Journal of Remote Sensing*, 57(1). <https://doi.org/10.1080/22797254.2022.2097450>
26. Mallick, B., Ahmed, B., & Vogt, J. (2017). Living with the risks of cyclone disasters in the south-western coastal region of Bangladesh. *Environments*, 4(1), 13.
27. Samanta, S., Hazra, S., Mondal, P. P., Chanda, A., Giri, S., French, J. R., & Nicholls, R. J. (2021). Assessment and attribution of Mangrove Forest changes in the Indian Sundarbans from 2000 to 2020. *Remote Sensing*, 13(24), 4957.

